Adsorption of Methyl Orange on Corncob Activated Carbon: Kinetic, Equilibrium, and Thermodynamic Studies

Abollé Abollé[1], Kouakou Yao Urbain[2], Kambiré Ollo[2,*],
Koné Yetchié Tchonrontcha[1] and Kouakou Adjoumani Rodrigue[1]

[1] Laboratoire de Thermodynamique et Physico-Chimie du Milieu, UFR Sciences Fondamentales et Appliquées, Université Nangui Abrogoua, 02 BP 801 Abidjan 02, Côte d'Ivoire

[2] UFR Sciences et Technologies, Université de Man, BP 20 Man, Côte d'Ivoire

[*] Corresponding author' email: kambireollo@yahoo.fr

Abstract

H_3PO_4 activated corncob carbon was used for removal of methyl orange. Characterization of the prepared carbon showed that it has many pores with a specific surface area equal to 714 m^2 g^{-1}. During this study, the concentration of methyl orange was monitored using a UV-visible spectrophotometer. The kinetic study of the adsorption of methyl orange on activated carbon was performed and the adsorption rate was found to be consistent with pseudo-second order kinetics with 240 min as the equilibrium time. The equilibrium adsorption revealed that the experimental data better fit the Langmuir isotherm model for methyl orange removal. It is noted that for optimal removal of 10 mg L^{-1} methyl orange in a 25 mL volume, 0.3 g of activated carbon and a pH equal to 2.04 are required. The maximum monolayer adsorption capacity for methyl orange removal was found to be 107.527 mg g^{-1}. Analysis of thermodynamic parameters showed that the adsorption process of methyl orange on activated carbon is physisorption, spontaneous and endothermic.

1. Introduction

Water has always been the engine of life on earth. However, it can sometimes become a real instrument of death when it is polluted and when it carries and spreads micro-organisms and chemical substances from the textile, cosmetics, plastic, paper,

pharmaceutical industries, etc. [1,2]. Chemicals such as dyes in wastewater are often difficult to biodegrade and the lack of or inadequate treatment systems leads to their accumulation in the water cycle [3]. These dye compounds can be carcinogenic and mutagenic and can cause serious human health problems [4]. Thus, the presence of organic pollutants or dyes in aqueous effluents is a major environmental concern. The fight against this environmental pollution requires the use of all necessary means to reduce the pollution to a minimum or to mitigate its effects. These pollutions of all kinds, waters and soils require the increased reinforcement of the techniques of fight [5].

The application of the regulations fixing the limit contents of undesirable substances in liquid effluents has led to the development of various techniques such as advanced oxidation processes, solvent extraction, adsorption, membrane filtration etc. [6-10].

Adsorption using activated carbon remains one of the most widely used techniques. Adsorption processes have been widely used in water and wastewater related industries [11-14]. Adsorption on activated carbons is usually used in dye removal due to its greater ability to remove chemical components [4]. This is due to the large surface area of activated carbon, its porous and chemically suitable characteristics [12]. However, commercial activated carbon is expensive due to the high cost of the starting raw material. For this reason, various types of research have been conducted on the preparation of activated carbon from low-cost available raw materials, including agricultural by-products such as sawdust, banana peels, corn cob waste [13,15].

Corn cob waste or corn cobs are by-products obtained after the consumption of corn kernels. Corn cobs do not swell clearly in water and do not decompose when contact with water is delayed. Therefore, they constitute an environmental problem. The main objective of this work is to produce activated carbons based on corn cobs capable of adsorbing methyl orange (MO). To achieve this, we set the specific objectives of preparing and characterizing activated carbons based on corn cobs and determining the optimal conditions for adsorption.

2. Material and Method

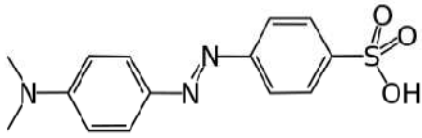### 2.1. Preparation of the corncob activated carbon

For the preparation of the activated carbon, corn cobs were used as precursor. The corn cobs were collected in the city of Korhogo (City located in the north of Côte d'Ivoire). The corn cobs were crushed into small pieces, washed with tap water to remove

dust and with distilled water and then dried at 105°C in an oven for 24 hours. The dried material is carbonized in an oven at 400° C for 2 hours. The resulting product is cooled to room temperature, crushed with a grinder, sieved (size ≤ 125 µm) to homogenize the particle size. The crushed product is then impregnated with the chemical agent (H_3PO_4 2 M) for 24 hours. The impregnated samples are oven dried at l05°C until complete evaporation of the impregnation liquid and then washed with distilled water under agitation until the pH of the rinse water is between 6 and 7. Finally, the samples are dried in an oven at 105°C for 24 hours.

2.2. Adsorbat studied

Methyl orange (C.I Acid Orange 52) otherwise known as Helianthine or orange III is a mainly acidic anionic dye. It is a color indicator used mainly for printing textile dyeing, but also in chemistry. Table 1 summarizes the properties of methyl orange (MO). A stock solution of MO (50 mg L^{-1}) was prepared by dissolving an appropriate amount of dehydrated MO (analytical grade, Sigma-Aldrich®). Experimental solutions of desired initial concentrations were obtained by diluting the MO stock solution with distilled water.

Table 1. Characteristics of MO.

Name	Methyl orange (C.I. 13025) PA-ACS
Family	Acid dye
Formula	$C_{14}H_{14}N_4NaO_3S$
Structure	
Molar mass	327.336
λ_{max}	465 nm
Solubility	5.2 g L^{-1} in water at 20°C; 1.0 g L^{-1} in ethanol at 20°C

2.3. Characterization of activated carbon

Surface functions were determined and quantified using the Boehm titration method by action of activated carbon on $NaHCO_3$, $CaCO_3$, NaOH and HCl [16].

The procedure used for the determination of the iodine value is an adaptation of the CEFIC 1989 method and the AWWA B 600-90 standard [17].

The specific surface area was determined by adsorption of acetic acid in aqueous medium on the active surface of activated carbon [14,18].

The ash content of the activated carbon was determined by reference to the American Standards Technology Method (ASTM), ASTM D 2866-94 [19]. A mass of activated carbon was heated to 650°C in the furnace until there was no detectable loss of mass. Calcination was carried out for 7 h.

The morphology of the activated carbon was determined by scanning electron microscope (SEM, ZEISS, SUPRA 40VP).

2.4. Adsorption tests in aqueous solution

The kinetic study was performed by placing 0.1 g of activated carbon with 25 mL of MO (10 mg/L) in an Erlenmeyer flask. The mixture was stirred with a magnetic stirrer at 25°C for times ranging from 0 min to 300 min. Regarding the study of parameters such as initial MO concentration, pH, activated carbon mass and temperature, one parameter is varied while fixing the other parameters. The mixture is stirred with a magnetic stirrer for 4 h.

The concentration of MO was monitored using a UV-visible spectrophotometer (HACH DR 6000). The adsorption rate (% adsorption) of MO on the activated carbon, is obtained according to the following formula:

$$\text{Adsorption rate}, \% = \frac{(C_0 - C_t)}{C_0} \times 100 \qquad (1)$$

With: C_0: initial concentration of MO (mg L^{-1}); C_t: residual concentration of MO at equilibrium (mg L^{-1}).

2.5. Theories

2.5.1. Modeling of adsorption kinetic

Pseudo-first-order and pseudo-second-order were used to investigate the MO adsorption kinetics on activated carbons. The linear form of the pseudo-first-order is given by the following equation [20-22]:

$$Ln(q_e - q_t) = Ln(q_e) - k_1 t \qquad (2)$$

where q_e and q_t (mg/g) are the amounts of the MO adsorbed at equilibrium and at time t (min), respectively, and k_1 (min) the rate constant for the pseudo-first-order rate.

The kinetics of the pseudo-second-order model was described by using the following equation [22,23]:

$$\frac{1}{q_t} = \frac{1}{k_2 q_e^2} \frac{1}{t} + \frac{1}{q_e} \tag{3}$$

where k_2 (g/mg/min) is the rate constant for the pseudo-second-order rate equation.

The linear form of the intraparticle diffusion models is given by the following equation [23] :

$$q_t = k_i t^{1/2} \tag{4}$$

where q_e and q_t are respectively the amount of MO adsorbed per mass of activated carbon at equilibrium time and at a time t in mg g^{-1}; k_1 / min^{-1}, k_2 / g mg^{-1} min^{-1}, and k_i / g mg^{-1} min$^{-1/2}$ the adsorption rate constant.

2.5.2. Adsorption isotherm models

Langmuir and Freundlich adsorption models were used to describe the experimental data of adsorption isotherms. The model developed by Langmuir is represented by the linear equation [22-24]:

$$\frac{1}{q_e} = \frac{1}{q_m} + \frac{1}{q_m b} \times \frac{1}{C_e} \tag{5}$$

where C_e is the equilibrium concentration (mg/L), q_e is the amount of adsorbate adsorbed per unit mass of the adsorbent at equilibrium (mg/g), b is the Langmiur adsorption constant (L/mg), and q_m is the maximum amount per unit mass of adsorbent (mg/g).

The general form of the Freundlich equation is given by Eq. (6) [22, 23]:

$$q_e = K_f C_e^{1/n} \tag{6}$$

where q_e is the quantity of solute adsorbed at equilibrium (mg/g), C_e is the concentration at equilibrium (mg/L), and K_f and n are the empirical constants.

The linear form is given by Eq. (7) [22, 23]:

$$\ln q_e = \ln K_f + \frac{1}{n} \ln C_e. \tag{7}$$

3. Results and Discussion

### 3.1. Characterization of activated carbon by scanning electron microscopy

The activated carbon was characterized by scanning electron microscopy before and after the adsorption of MO on its surface. The resulting images are shown in Figure 1a and 1b. Before adsorption of MO, the activated carbon shows a large number of open and irregular pores on its surface. The presence of these pores is due to the activation of the carbon. The image obtained after adsorption of MO shows a reduction in the size of the micropores. This is due to the attachment of the MO molecules inside the micropores. In addition, there are pits on the carbon surface. The methyl orange molecules after filling the pores are bound to the carbon surface giving an almost smooth surface. There was thus a strong interaction between MO and activated carbon.
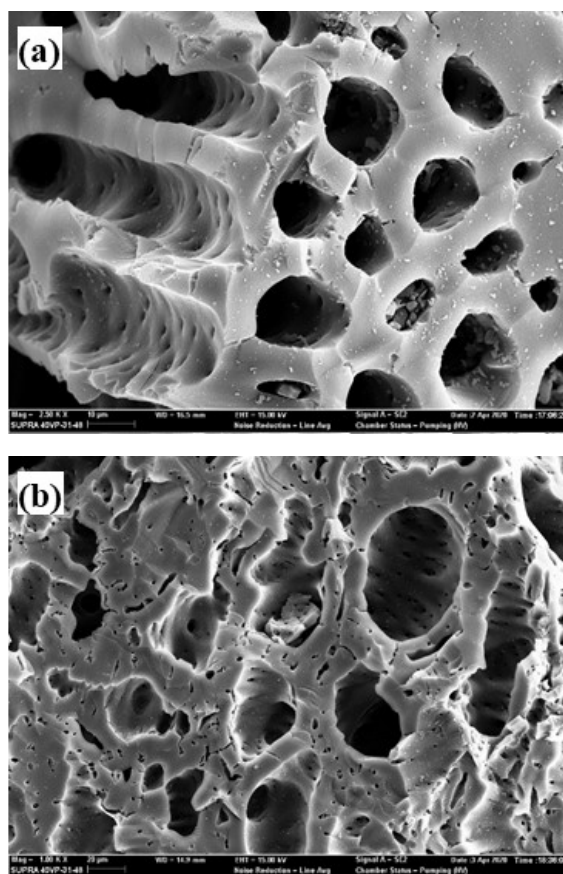
Figure 1. SEM image of activated carbon (a) and after adsorption of MO (b).

3.2. Characterization of activated carbon by specific surface

Acetic acid as a model pollutant is used by some researchers to determine the specific surface of activated carbon in aqueous media [25]. This choice is justified by the specific surface of this molecule which is close to that of the diazote used for the determination of the specific surface by the BET method. In this work the specific surface was determined by acetic acid adsorption. The Langmuir isotherms obtained by plotting $q_e^{-1} = f(C_e^{-1})$ are those shown in Figure 2.
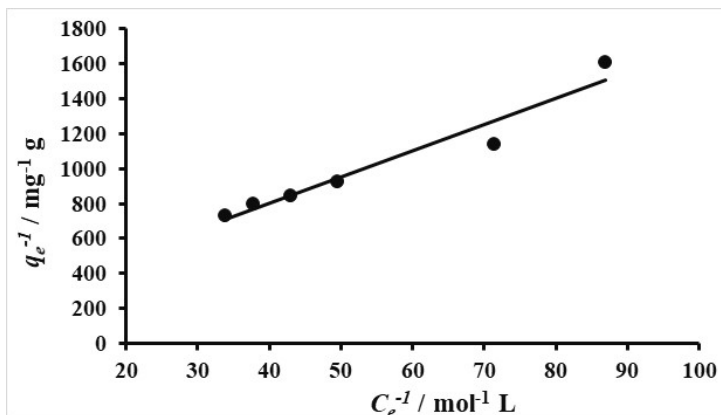
Figure 2. Application of the Langmuir model to the adsorption of acetic acid mass = 0.1 g, $T = 27°C$.

The different parameters obtained by adsorption of acetic acid on the different carbons as well as the specific surfaces of the carbons are grouped in Table 2. The value of the specific surface obtained is 714 m^2 g^{-1}.

Table 2. Parameter values of the Langmuir adsorption isotherm and the specific surface of the carbon.

R^2	q_m / mol g^{-1}	Specific Area (m^2 g^{-1})
0.972	5.34.10^{-3}	714

3.3. Ash content and iodine number

The iodine number is a measure of the micropore content of an activated carbon. The value obtained with the prepared activated carbon is 702 mg g^{-1} (Table 3). This table also shows that the ash content of the carbon is 4 %. This value shows that the carbon has a low fraction of mineral compounds and a high carbon fraction. These low values of ash

content are due on the one hand to the fact that the precursors of these carbons are vegetable matter and therefore less rich in mineral matter and, on the other hand, to the washing of the carbons after preparation which eliminated any ash that might be available. This reflects a good preparation of the carbon [23].

Table 3. Ash content and iodine number.

Ash content	iodine number
4 %	702 mg g^{-1}

3.4. Surface functions

The surface functions of activated carbon were determined. The results obtained are presented in Table 4. This table shows that activated carbon has a surface of functional groups with acidic (72.31%) and basic (27.69%) character. The presence of acidic and basic sites on the carbon suggests that it can adsorb both anionic and cationic adsorbates with a high proportion for cations [26]. The high acidity of carbon may be due primarily to chemical activation that increases the carboxyl function [27]. The basic sites are mainly of the Lewis type associated with π-electron rich regions located at the basal planes. The low value of the basic function on the surface of the carbon is due to the oxidation process.

Table 4. Normalities (meqg L^{-1}) of acid and base functions of activated carbons.

| Acid functions			Total acid functions	Total basic functions
Carboxylic	Lactone	Phenolic		
1.46	1.88	2.04	5.38	2.06
19.62 %	25.27 %	27.42 %	72.31 %	27.69 %

3.5. Adsorption kinetics of MO

The study of the influence of stirring time on the adsorption rate of MO was performed. The result obtained is presented in Figure 3a. It clearly appears that the adsorption of MO is fast up to 90 min. This step corresponds to the adsorption of MO on the most accessible sites, probably located on the external surfaces of the activated carbon particles [28,29]. After 90 min, the adsorption slowly increases and eventually reaches equilibrium after 240 min. This reflects a saturation of the carbon pores. A time of 240 min (4 hours) was therefore used as the equilibrium time for further work in our study. The rapid adsorption phenomenon observed at the beginning of contact means that

there is a large number of sites available for dye adsorption. But this can also be related to the physicochemical characteristics of the material and especially to the nature of the sites on the surface and the porosity of the material. The constant phase is due to the fact that the adsorption sites are more and more occupied, thus becoming less and less available, there follows a diffusion towards the less accessible sites slowing down the adsorption rate before reaching the equilibrium state. Adsorption rates of 88.14 and 96.44% were obtained after 90 and 240 min of adsorption respectively.

In an effort to determine which kinetic model best describes the adsorption of methyl orange onto activated carbon, the pseudo-first order reaction, pseudo-second order reaction, and intraparticle diffusion models were applied, using equations 2, 3, and 4, respectively.

The plotted curves are $ln(q_e - q_t)$ versus time, tq_t^{-1} versus time, and q_t versus $t^{1/2}$, respectively. The results obtained are shown in Figure 3b, 3c and 3d. The rate constants and linear correlation coefficients are reported in Table 5.
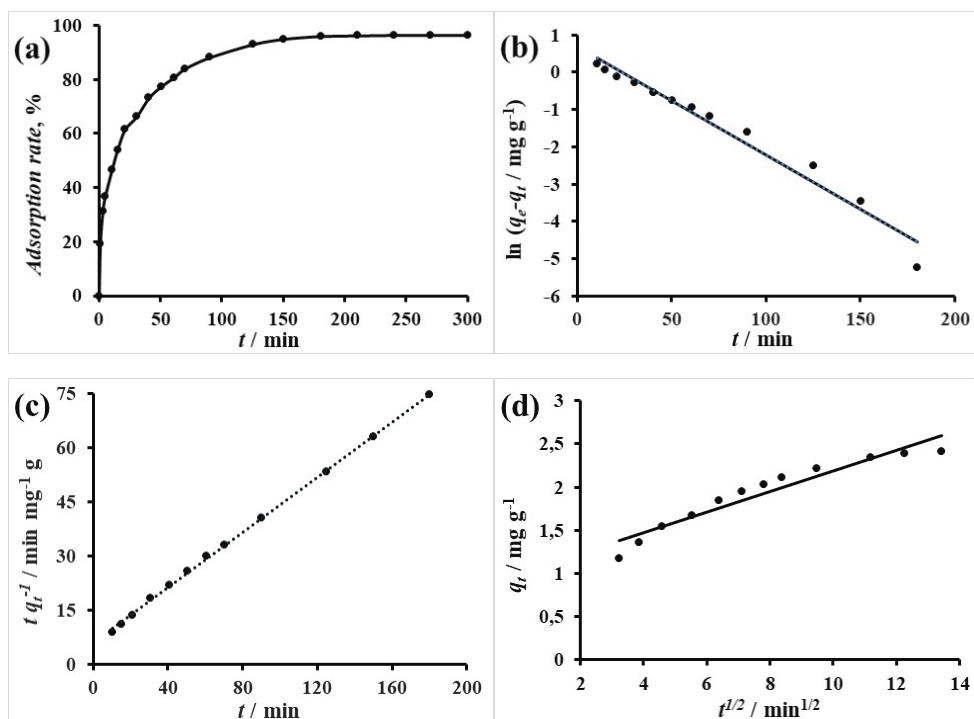
Figure 3. Removal efficiencies of MO on activated carbon (a); Application of pseudo-first order (b); pseudo-second order (c) and intraparticle diffusion (d) kinetic model to MO adsorption, activated carbon mass = 0.1 g; [MO] = 10 mg L^{-1}.

The results in Table 5 indicate that the coefficients of determination are 0.961; 0.999 and 0.923 for the pseudo-first order model and the pseudo-second order model and the intraparticle diffusion model respectively. This shows that the kinetic model which best describes the adsorption of MO on activated carbon is the pseudo-second order model. A kinetic model of pseudo-second order was also obtained with the adsorption of methyl orange on biosorbents [30, 31]. The adsorption would be a bimolecular process consisting of a collision between a MO molecule and an adsorption site.

Table 5. Parameters of the methyl orange adsorption kinetics models.

Pseudo-first order		Pseudo-second order		Intraparticle diffusion	
R^2	k_1/ min^{-1}	R^2	k_2 / g mg^{-1} min^{-1}	R^2	k_i / g mg^{-1} min$^{-1/2}$
0.961	0.029	0.999	0.028	0.923	0.119

3.6. Influence of the initial concentration of MO and modeling of adsorption isotherms

The adsorption isotherm provides indications on the nature of the adsorbate-adsorbent interactions as well as on the characteristics of the adsorbate. It was performed at 25°C for 240 min corresponding to the equilibrium time. Figure 4 shows the adsorption isotherm of MO on activated carbon.

This isotherm is similar to the IUPAC type I. This type of isotherm is observed in the case of strong interactions between adsorbent and adsorbate and that of physical adsorption in microporous solids. Activated carbon being microporous, this type of isotherm is commonly obtained by researchers [32]. A progressive saturation of the pores of the carbon is noted.

In order to model the adsorption phenomenon, Freundlich and Langmuir models were used. If the graphical representation of $ln\ q_e$ as a function of $ln\ C_e$ gives a straight line, we can conclude that the Freundlich equation is applicable. This allows us to calculate the constants k and n [33].

The Langmuir model is used to calculate the maximum adsorption capacity of adsorbent materials [11].

Applied to our experimental results the Freundlich and Langmuir models give Figure 4b and 4c. The parameters obtained are recorded in Table 6.

Table 6. Parameters of the Langmuir and Freundlich equations.

Freundlich			Langmuir		
R^2	$\ln K_f$	n	R^2	q_m /mg g^{-1}	b
0.973	0.101	1.318	0.996	107.527	0.270

Both models are applicable, but the Langmuir model describes better this adsorption because its correlation coefficient is closer to 1. This shows that the sites are equivalent (uniform surface), we have the formation of a monolayer and there is no interaction between the adsorbed molecules.

The maximum adsorption capacity of this carbon towards methyl orange is 107.527 mg g^{-1}.
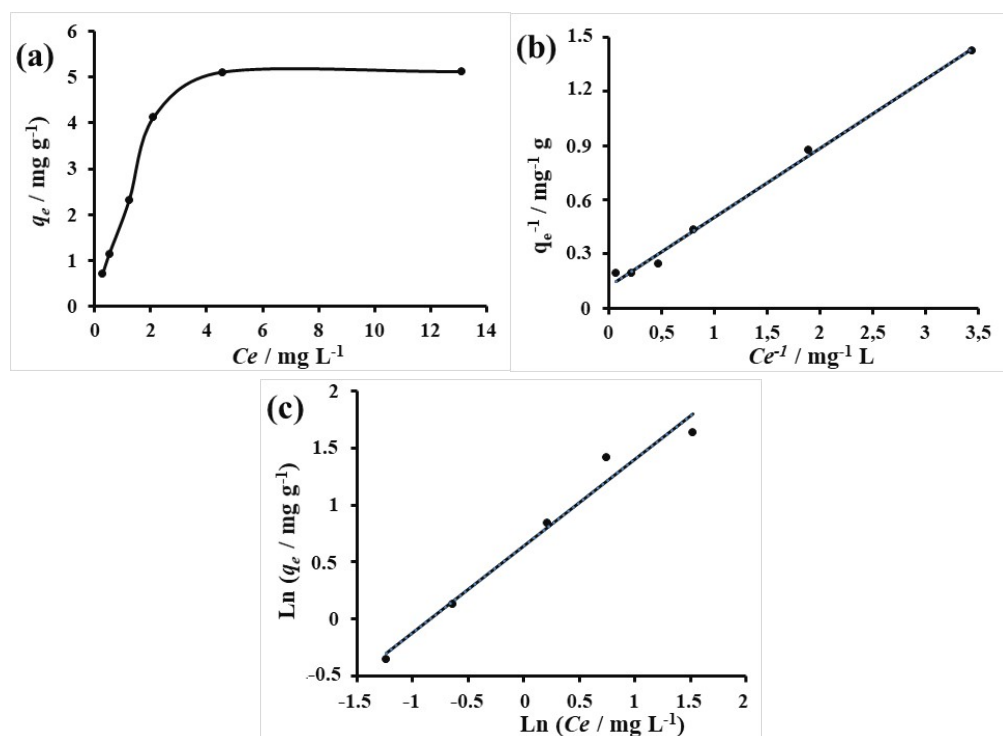
Figure 4. Adsorption isotherms of MO on activated carbon (a), Langmuir model (b) and Freundlich model (c) applied to MO adsorption; carbon mass = 0.1g.

The maximum monolayer adsorption capacity (q_{max}) values obtained for the adsorption of MO onto corn cobs activated carbon in our study were compared with those obtained by using other adsorbents (Table 7). The amount of OM adsorbed on our coal is higher than the results of the work recorded in Table.

Table 7. Adsorption capacities of MO on various adsorbents.

Adsorbent	Maximum adsorbent capacity, q_{max} (mg.g^{-1})	References
Mango seed kernels	5.71	[34]
AgNPs-coated AC	27.48	[35]
Modified halloysite nanotubes	94.34	[36]
Swietenia mahagoni bark activated carbon	6.071	[37]
Corncobactivated carbon	107.527	This study

3.7. Influence of activated carbon mass on the adsorption of MO

The influence of carbon mass was investigated with the objective of determining the mass of carbon corresponding to an optimal adsorption rate of MO. Figure 5 shows the results obtained.
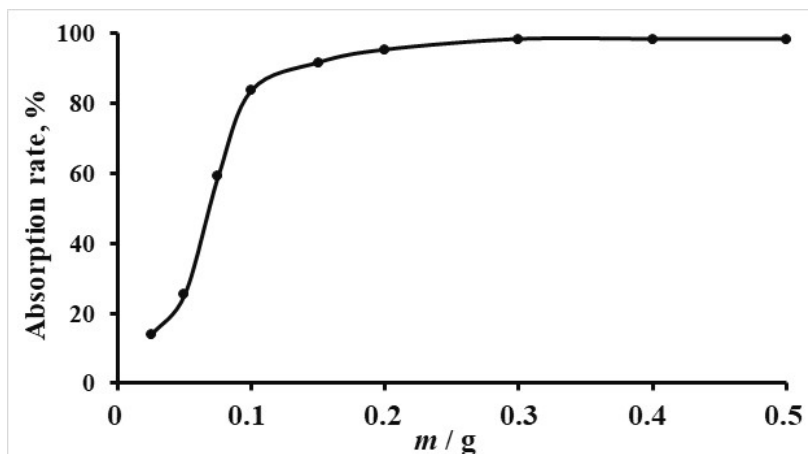

Figure 5. Influence of adsorbent mass on the adsorption of MO.

In this figure, a rapid change in the adsorption rate can be seen when the dose of activated carbon is varied from 0.025 g to 0.15 g L^{-1}. The adsorption rate for this dose variation increases from 13.94% to 91.73%. Above 0.15 g there is a slow increase in the adsorption rate of methyl orange which tends to a steady state at 98.42% from 0.3 g. The mass of the activated carbon therefore has an influence on the adsorption capacity of methyl orange. After a rapid growth, it shows a plateau reflecting saturation and thus the maximum adsorption amount.

3.8. Influence of pH on adsorption

The study of the influence of pH on adsorption was performed by varying the pH from 2.04 to 11.61 for a dose of 0.2 g of activated carbon in contact in 25 mL of methyl orange of concentration 10 mg L^{-1}. The pH values were adjusted by 0.1 M HCl and NaOH solutions. The results expressed in terms of adsorption rate versus pH are shown in Figure 6. The adsorption rate reaches the maximum values in very acidic environment. The removal rate values of 99.75%; 99.17%; 95.30%; 95.24% and 52.09% were obtained at pH = 2.04; 4.18; 6.5; 9.25 and 11.61 respectively. This shows that a decrease in the abatement rate is observed as the pH value increases. It is also noted that the removal efficiency is at its maximum for pH = 2.04.
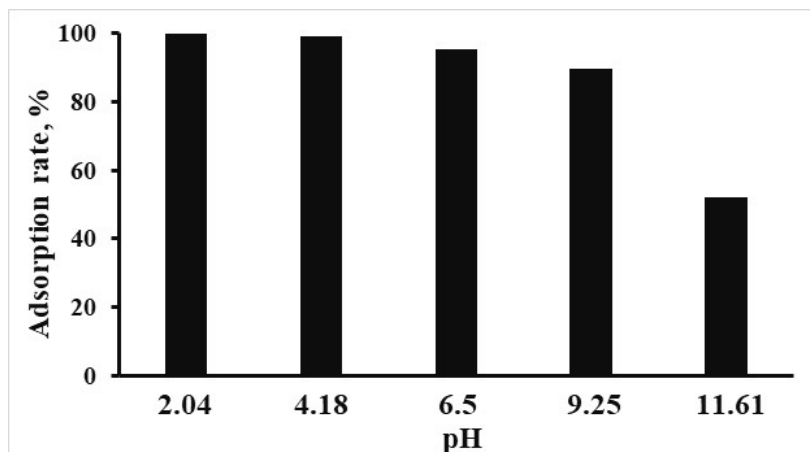
Figure 6. Influence of the initial pH on the adsorption of MO.

The pH of the solution of MO, an anionic dye, has an influence on the adsorption capacity. The work of some authors [14,38], on the removal of dyes in aqueous solution on activated carbon obtained from biomass has led to similar results. The latter indicate

that activated carbon presents positive charges on its surface. Indeed, an increase in pH leads to a greater hydrophilic character of organic compounds. At acidic pH, the number of positively charged sites increases, favouring the adsorption of anions by the phenomenon of electrostatic attraction.

The decrease in the adsorption rate of MO with the increase of the pH value in alkaline medium could be explained by an excess of OH⁻ ions in the medium which leads to a competition with the anionic dye on the adsorption sites of the activated carbon. Indeed, the high concentration and the high mobility of OH⁻ ions favor their adsorption compared to the anionic dye.

3.9. Thermodynamic adsorption properties

The thermodynamic parameters of the adsorption reaction of methyl orange on CAZ, namely the standard free enthalpy ($\Delta G°$), standard enthalpy ($\Delta H°$) and standard entropy ($\Delta S°$) were determined from equations (8), (9) and (10) [38]:

$$\Delta G° = \Delta H° - T\Delta S° \qquad (8)$$

It is related to the constant of the mass action law (K') by a relation of the form :

$$\Delta G = -RT \ln K' \qquad (9)$$

In the case of the adsorption reaction the equilibrium constant (K') can be assimilated to the distribution coefficient K_d of the solute between the solid phase (adsorbent) and the liquid phase (solution).

We can therefore write:

$$\Delta G° = - RT \ln K_d \qquad (10)$$

with $K_{dis} = C_S/C_L$

C_S = concentration of MO in the solid phase; C_L = concentration of MO in the liquid phase. Or taking into account the following relation:

$$\text{Ln } K_d = \Delta S°/R - \Delta H°/RT \qquad (11)$$

Figure 7 shows the curve of $Ln (K_d)$ versus T^{-1} for the adsorption of MO on carbon. The values of enthalpy and standard entropy deduced from the slope and intercept, respectively, represent $ln K_d$ as a function of $f(T^{-1})$ are grouped in Table 8.

Table 8. Thermodynamic parameters.

$\Delta H°$ / J mol^{-1}	16170.04			
$\Delta S°$ / J mol^{-1} K^{-1}	64.22			
$\Delta G°$ / J mol^{-1}	298.15 K	314.15 K	323.95 K	329.55 K
	-2977.15	-4004.67	-4634.03	-4993.661

Analysis of these thermodynamic parameters showed that the adsorption process of the adsorbate (MO) on the adsorbent (carbon) proceeds as a spontaneous reaction, regardless of the temperature ($\Delta G° < 0$) [6]. The change in free enthalpy ($\Delta G°$) changes inversely with the solution temperature. Thus, increasing temperature further favors the adsorption process of MO on activated carbon. The positive sign of the standard enthalpy $\Delta H°$, confirms that the adsorption process is endothermic. The calculated value of $\Delta H°$ is less than 40 kJ mol^{-1}. This result shows that it is a physisorption [6]. The positive sign of the entropy ($\Delta S°$) indicates disordering of the MO molecules at the solid-solution interface during the adsorption process [6].
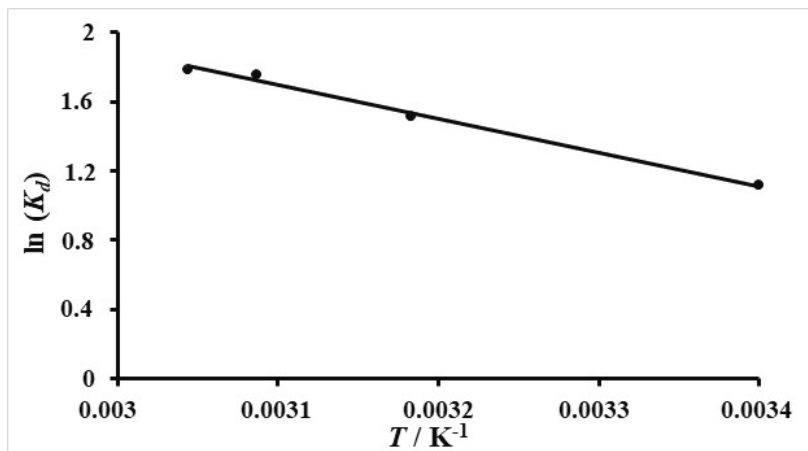
Figure 7. Curve of $Ln(K_d)$ versus T^{-1} for the adsorption of MO on activated carbon.

4. Conclusion

Characterization of the prepared charcoal showed that it has many micropores. The specific surface area obtained is equal to 714 m^2 g^{-1} showing that the zinc chloride activated carbon has a large specific surface area. Kinetic study of the adsorption of methyl orange on zinc chloride activated carbon was carried out and the adsorption rate

was found to be in accordance with pseudo-second order kinetics with 240 min as equilibrium time. Equilibrium adsorption revealed that the experimental data fit the Langmuir isotherm model better. The maximum monolayer adsorption capacity for MO removal was found to be 107.527 mg g^{-1}. The study of the influence of the pH of the initial solution showed that the rate of methyl orange adsorption removal is observed at pH = 2.04. The analysis of thermodynamic parameters showed that the adsorption process of MO on carbon is physisorption, spontaneous and endothermic.

Conflicts of Interest

The authors declare that there is no conflict of interest.

References

[1] Wang, Q., & Yang, Z. (2016). Industrial water pollution, water environment treatment, and health risks in China. *Environmental Pollution, 218*, 358-365. https://doi.org/10.1016/j.envpol.2016.07.011

[2] Adeleke, A., Olumuyiwa, O., Mutiu, S., Kafeelah, Y., Ojo, O., Bernadine, E., Iyabode, A., Bamitale, F., & Olubunmi, A. (2020). Quantification of metal contaminants and risk assessment in some urban watersheds. *J. Water Res. Protec.*, *12*, 951-963. https://doi.org/10.4236/jwarp.2020.1211056

[3] Sagnik, C., Anupam, S., Subhabrata, M., Naga, D., Saima, R.M., Saima, I., & Papita, D. (2021). Study on isotherm, kinetics, and thermodynamics of adsorption of crystal violet dye by calcium oxide modified fly ash Environ. *Eng. Res.*, *26*(1), 190372. https://doi.org/10.4491/eer.2019.372

[4] Rania, A.-T., Sameh, S.A., Fanghua, L., Kamal, M.O., Yehia, A.-G.M., Tamer, E., Haixin, J., Yinyi, F., & Jianzhong, S. (2022). A critical review on the treatment of dye-containing wastewater: Ecotoxicological and health concerns of textile dyes and possible remediation approaches for environmental safety. *Ecotoxicology and Environmental Safety*, *231*, 113160. https://doi.org/10.1016/j.ecoenv.2021.113160

[5] Chang, J.-S. (2001). Recent development of plasma pollution control technology: a critical review. *Science and Technology of Advanced Materials*, *2*(3-4), 571-576. https://doi.org/10.1016/S1468-6996(01)00139-5

[6] Coulibaly, B., Pohan, L.A.G., Kambiré, O., Kouakou, L.P.S., Goure-Doubi, H., Diabaté, D., & Ouattara, L. (2020). Valorization of green clay from Bouaflé (Ivory Coast) in the simultaneous elimination of organic pollutants and metallic trace elements by adsorption: Case of methylene blue and cadmium ions. *Chemical Science International Journal*, *29*(8), 37-51. https://doi.org/10.9734/CSJI/2020/v29i830200

[7]   Kambiré, O., Pohan, L.A.G., Sadia, S.P., Kouadio, K.E., & Ouattara, L. (2020). Voltammetric study of formic acid oxidation via active chlorine on IrO_2/Ti and RuO_2/Ti electrodes. *Mediterranean Journal of Chemistry*, *10*(8), 799-808. http://doi.org/10.13171/mjc10802010271525ko

[8]   Kambiré, O., Alloko, K.S.P., Pohan, L.A.G., Koffi, K.S., & Ouattara, L. (2021). Electrooxidation of the paracetamol on boron doped diamond anode modified by gold particles. *International Research Journal of Pure & Applied Chemistry*, *22*(4), 23-35. https://doi.org/10.9734/irjpac/2021/v22i430401

[9]   Berté, M., Quand-même, G.C., Ollo, K., Placide, S.S., Sylvestre, K.K., & Lassiné, O. (2022). Electrochemical behavior of paracetamol on thermally prepared $Ti/Ta_2O_5/_{50}Pt$-$_{50}RuO_2$ electrode. *Mediterranean Journal of Chemistry*, *12*(1), 38-50. http://dx.doi.org/10.13171/mjc02205131627berté-lassiné

[10] Kouadio, K.E., Kambiré, O., Koffi, K.S., & Ouattara, L. (2021). Electrochemicaloxidation of paracetamol on boron-doped diamond electrode: analytical performance and paracetamol degradation. *J. Electrochem. Sci. Eng., 11*(2), 71-86. https://doi.org/10.5599/jese.932

[11] Sukmana, H., Bellahsen, N., Pantoja, F., & Hodur, C. (2021). Adsorption and coagulation in wastewater treatment – Review. *Progress in Agricultural Engineering Sciences*, *17*(1), 49-68. https://doi.org/10.1556/446.2021.00029

[12] Wei, M., Marrakchi, F., Yuan, C., Cheng, X., Jiang, D., Zafar, F.F., Fu, Y., & Wang, S. (2022). Adsorption modeling, thermodynamics, and DFT simulation of tetracycline onto mesoporous and high-surface-area naoh-activated macroalgae carbon. *Journal of Hazardous Materials*, 425, 127887. https://doi.org/10.1016/j.jhazmat.2021.127887

[13] Syieluing, W., Nawal, A.G., Norzita, N., Fatin, A.R., Ibrahim, M.I., Ramli, M., & Nor, A.S.A. (2020). Effective removal of anionic textile dyes using adsorbent synthesized from coffee waste. *Waste. Sci Rep., 10*, 2928. https://doi.org/10.1038/s41598-020-60021-6

[14] Kambiré, O., Kouakou, Y.U., Kouyaté, A., Sadia, S.P., Kouadio, K.E., Kimou, K.J., & Koné, S. (2021). Removal of rhodamine B from aqueous solution by adsorption on corn cobs activated carbon. *Medite. J. Chem*., *11*, 271-281. http://doi.org/10.13171/mjc02112131596ollo

[15] Ramutshatsha-Makhwedzha, D., Mbaya, R., & Mavhungu, M.L. (2022). Application of activated carbon banana peel coated with Al_2O_3-Chitosanfor the adsorptive removal of lead and cadmium from wastewater. *Materials*, *15*, 860. https://doi.org/10.3390/ma15030860

[16]   Boehm, H.P. (1994). Some aspects of the surface chemistry of carbon blacks and other carbons. *Carbon.*, *32*, 759-769. https://doi.org/10.1016/0008-6223(94)90031-0

[17]   CEFIC (Conseil européen de l'industrie chimique) (1989). Méthodes de contrôle et d'évaluation des charbons actifs.

[18]   Hamouz, A.E., Hilal, H.S., Nashaat, N., & Zahi, M. (2007). Solid olive waste in environmental clean-up: oil recovery and carbon production for water purification. *Journal of Environmental Management, 84*, 83-92. https://doi.org/10.1016/j.jenvman.2006.05.003

[19]   ASTM D2866-94 (1999). Standard Test Method for Total Ash Content of Activated Carbon.

[20]   Lagergren, S. (1898). About the theory of so-called adsorption of soluble substances. *Kungliga Svenska Vetensk Handl*, *24*, 1-39.

[21]   Ho, Y.S., & McKay, G. (1999). Pseudo-second order model for sorption processes. *Process Biochem*, *34*, 451-465. https://doi.org/10.1016/S0032-9592(98)00112-5

[22]   N'goran, K.P.D.A., Diabaté, D., Yao, K.M., Kouassi N.L.B., Gnonsoro, U.P., Kinimo, K.C., & Trokourey, A. (2018). Lead and cadmium removal from natural freshwater using mixed activated carbons from cashew and shea nut shells. *Arabian Journal of Geosciences, 11*, 498. https://doi.org/10.1007/s12517-018-3862-2

[23]   Kouakou, Y.U., Essy, K.F., Dembele, A., Brou, Y.S., Ello, S.A., Gouli Bi, I.M., & Trokourey, A. (2017). Removal of imidacloprid using activated carbon produced from ricinodendronheudelotii shells. *Bull. Chem. Soc. Ethiop., 31*(3), 397-409. http://dx.doi.org/10.4314/bcse.v31i3.4

[24]   Langmuir, I (1906). The adsorption of gases on plane surfaces of glass, mica and platinum. *J. Am. Chem. Soc., 40*, 1361-1403.

[25]   El-Hamouz, A., Hilal, H.S., Nassar, N., & Mardawi, Z. (2007). Solid olive waste in environmental cleanup: Oil recovery and carbon production for water purification. *Journal of Environmental Management*, *84*, 83-92. https://doi.org/10.1016/j.jenvman.2006.05.003

[26]   Altenor, S., Carene, B., Emmanuel, E., Lambert, J., Ehrhardt, J.J., & Gaspard, S. (2009). Adsorption studies of methylene blue and phenol onto vetiver roots activated carbon prepared by chemical activation. *Journal of Hazardous Materials*, *165*, 1029-1039. https://doi.org/10.1016/j.jhazmat.2008.10.133

[27]   Wang, S., & Zhu, Z.H. (2007). Effects of acidic treatment of activated carbons on dye adsorption. *Dyes and Pigments*, *75*(2), 306-314. https://doi.org/10.1016/j.dyepig.2006.06.005

[28] Singh, N., Kloeppel, H., & Klein, W. (2001). Sorption behavior of metolachlor, isoproturon, and terbuthylazine in soils. *Journal of Environmental Science and Health, Part B*, *36*, 397-407. https://doi.org/10.1081/PFC-100104184

[29] Gao, J.P., Maghun, J., Spitzauer, P., & Kettrup, A. (1998). Sorption of pesticides in the sediment of the Teufelsweiher pond (Southern Germany). I: Equilibrium assessments, effect of organic carbon content and pH. *Water Reseach.*, *32*, 1662-1672. https://doi.org/10.1016/S0043-1354(97)00377-1

[30] Ramakrishnan, R.K., Padil, V.V.T., Wacławek, S., Černík, M., & Varma, R.S. (2021). Eco-friendly and economic, adsorptive removal of cationic and anionic dyes by bio-based karaya gum—chitosan sponge. *Polymers*, *13*, 251. https://doi.org/10.3390/polym13020251

[31] Munagapati, V.S., & Dong-Su, K. (2016). Adsorption of methyl orange from aqueous solution by aminated pumpkin seed powder: Kinetics, isotherms, and thermodynamic studies. *Ecotoxicology and Environmental Safety*, *128*, 109-117. http://dx.doi.org/10.1016/j.ecoenv.2016.02.016

[32] Mardini, F.A., & Legube, B. (2009). Effect of the adsorbate (Bromacil) equilibrium concentration in water on its adsorption on powdered activated carbon. Part 1. Equilibrium parameters. *Journal of Hazardous Materials*, *170*, 744-753. https://doi.org/10.1016/j.jhazmat.2009.05.003

[33] Carvalho, M.F., Duque, A.F., Goncalves, I.C., & Castro, P.M.L. (2006). Adsorption of fluorobenzene onto granular activated carbón: isotherm and bioavailability studies. *Bioresource Technology*, *98*, 3423-3430. https://doi.org/10.1016/j.biortech.(2006).11.001

[34] Khelifi, O., Mehrez, I., Younsi, M., Nacef, M., & Affoune, A. (2018). Methylorange adsorption on biosorbent derived from mango seed kernels. *Larhyss Journal*, *36*, 145-156.

[35] Jolly, P., Manas, K.D., Dhananjay, K.D., & Devsharan, V. (2013). Removal of methyl orange by activated carbon modified by silver nanoparticles. *Appl Water Sci*, *3*, 367-374. https://doi.org/10.1007/s13201-013-0087-0

[36] Liu, R., Fu, K., Zhang, B., Mei, D., Zhang, H., & Liu, J. (2012). Removal of methyl orange by modified halloysite nanotubes. *J Dispersion Sci Technol.*, *33*, 711-718. https://doi.org/10.1080/01932691.2011.579855

[37] Ghosh, G.C., Chakraborty, T.K., Zaman, S., Nahar, M.N., & Kabir, A.H.M.E. (2020). Removal of methyl orange dye from aqueous solution by a low cost activated carbon prepared from Mahagoni (Swietenia mahagoni) bark. *Pollution*, *6*(1), 171-184, https://doi.org/10.22059/poll.2019.289061.679

[38] Sultana, M., Rownok, M.H., Sabrin, M., Rahaman, M.H., & Alam, S.M.N. (2022). A review on experimental chemically modified activated carbon to enhance dye and heavy metals adsorption. *Cleaner Engineering and Technology*, *6*, 100382. https://doi.org/10.1016/j.clet.2021.100382